

Nonexponential dynamic relaxation of randomly branched polymers in good solvents

Josh Kemp and Zheng Yu Chen

*Guelph-Waterloo Program for Graduate Work in Physics and Department of Physics, University of Waterloo,
Waterloo, Ontario, Canada N2L 3G1*

(Received 6 August 1997)

Monte Carlo simulations were carried out to study the dynamics of randomly branched polymers in good solvents. Two types of time scales were observed: fast relaxation times corresponding to the internal contraction motions and slower relaxation times corresponding to the overall rotational motions of the polymers. The former is associated with autocorrelation functions that exhibit nonexponential decay behavior, a signature of the dynamics of random systems. The latter is associated with the usual exponential decay behavior, typical of linear or regularly branched polymers. [S1063-651X(97)04912-X]

PACS number(s): 61.25.Hq, 61.20.Ja, 64.60.Ht

A wide range of naturally occurring and artificially synthesized polymers have randomly branched structures [1,2] (see Fig. 1 for a sketch). The dynamic relaxations of various autocorrelation functions are important measurements used to understand the microscopic motion of polymers under different physical conditions. For polymers of any structure moving in a good solvent, the overall motion of the entire polymer can be quantitatively described by the diffusive motion of an object of radius S , where S is a characteristic radius of the polymer. The internal relaxation modes, connected to the internal degrees of freedom, are closely connected to the structure of the molecule and are usually different from one type of polymer to another. The randomness in the structure of randomly branched polymers produces an interesting yet complex feature: The autocorrelation functions associated with internal degrees of freedom could exhibit, as observed in the current study, a nonexponential relaxation that is characteristic of many other randomly disordered systems such as spin glasses [3] and randomly sequenced, proteinlike polymers [4]. Despite current interest in randomly branched polymers (RBP's) [1,2,5-9], the dynamics of such molecules is not completely understood. In this paper we present our recent results on the numerical simulations of the Rouse dynamics of RBP's.

Bearing some similarities to RBP's are regularly branched polymers such as star and comblike polymers: All have overall spherical conformation and more than one relaxation time. Grest and Murat studied the dynamics of f -arm star polymers numerically by implementing a molecular-dynamics (MD) simulation method [10]. In particular, they have proposed characterizing the dynamic relaxation process by using three different time scales: the elastic relaxation time τ_{el} , rotational relaxation time τ_{rot} , and entanglement relaxation time τ_{ent} . These relaxation times are expected to be short (τ_{el}), long (τ_{rot}), and ultralong (τ_{ent}) due to the different physical mechanisms involved. The MD simulations produced numerical results for observing the elastic time scale, but did not yield enough statistics for observing the other two time scales for which a scaling argument is available. Su, Denny, and Kovac studied the dynamics of star polymers by using the bond-fluctuation Monte Carlo (MC) model, focusing mainly on the relaxation phenomena of shape fluctuations [11]. The elastic relaxation times were

also determined and compared with scaling laws. In addition, they tried to analyze the simulation data for the overall rotation of the molecules. Unfortunately, the time duration of the observation was not long enough for a conclusive determination of the relaxation behavior associated with the rotational motion. In this study, we examined the dynamic relaxations of RBP's at both short- and long-time scales.

For regularly branched or linear polymers, the analytic calculation of various relaxation times is strongly related to the identification of the primary normal-mode vibrations of the molecule in the θ condition [12]. As early as 1959, Zimm and Kilb studied the normal mode relaxation time of star polymers in the θ condition [13]. Recently, this has also been done for star-burst polymers by Cai and Chen [14]. The introduction of the excluded-volume interaction may significantly alter the scaling relation between, for example, τ and the total number of monomers N , but the new τ 's can always be traced back to their θ condition counterpart. There is no previous theoretical determination of the relaxation phenomena in RBP's, even for the simplest case of a phantom polymer in the θ condition. The main difficulty is conceptual: How does one identify the normal modes for a randomly structured object? Computer simulations, however, can avoid such difficulties by directly observing various autocorrelation functions numerically.

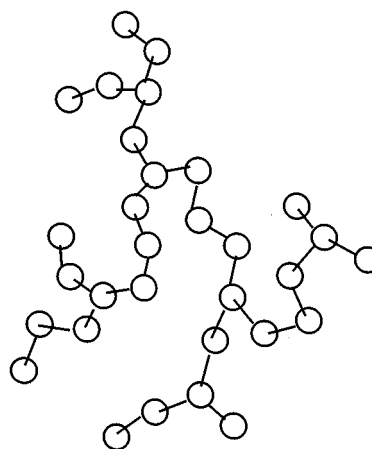


FIG. 1. Sketch of a typical randomly branched polymer.

The goal of this study is to examine the dynamics of annealed RBP's containing various numbers of monomers and to find the relevant scaling behavior. The simulation of the dynamics of these structures has proved particularly challenging as the dynamic behavior of each polymer depends on its particular branching structure. In principle, for a given N , one would need to determine the autocorrelation functions for many uncorrelated sample structures and determine the structurally averaged autocorrelation function based on an average over these structures. We have used the simpler treatment of choosing only five independent representative structures for each N in our calculations.

The importance of the random structure to the static conformational properties of RBP's has been emphasized recently [5,6]. For the presentation of the dynamical properties below, we note that the mean-square radius of gyration obeys a scaling law $\langle S^2 \rangle \propto N^{2\nu}$, where $\nu=0.5$ for annealed polymers [7,9] and $\nu=0.45$ for quenched polymers [6]. Because of the smaller gyration exponent ν compared to its linear-polymer counterpart ($\nu_{\text{linear}} \approx 0.6$), randomly branched polymers are much denser than linear polymers. The systems studied in this paper all have annealed structures.

The bond-fluctuation MC dynamics has been shown to effectively reflect the Rouse dynamics of actual systems [15] when the hydrodynamic interactions between different monomers are ignored (the draining limit). Since the volume interaction is automatically embedded in the bond fluctuation model, this method also qualitatively reproduces the physical environment of polymers in a good solvent.

We used an eight-site, three-dimensional bond-fluctuation algorithm to simulate the Rouse dynamics of the polymers. The algorithm was originally introduced by Carmenson and Kremer for simulating the dynamics of linear polymers; they also showed that the MC dynamics obtained in this way effectively mimic the true long-time molecular dynamics. Since a background cubic lattice system is adopted in this model, the faster integer manipulation of the algorithm makes it more favorable in comparison with other models. The model assumes that each monomer occupies one cube on the lattice and can be moved unit lengths along the six lattice directions. Moves are accepted when the bonds joining the monomers have lengths belonging to the set $l=2, \sqrt{5}, \sqrt{6}, 3, \sqrt{10}$ and when monomers do not overlap. The former constraint ensures that bonds will not cross each other, as shown by Carmenson and Kremer, while the latter accounts for the excluded-volume interaction between monomers. Interested readers are referred to Ref. [15] for a detailed description of the bond-fluctuation model.

The initial branching structures were built through an extension of the bond fluctuation model to include additional cutting and pasting steps to deal with the branching structures of annealed molecules. The procedure is similar to that used in the lattice-tree model of van Rensburg and Madras in their earlier study of the conformation properties of randomly branched polymers [7]. Starting from a linear chain of N monomers, we chose a free end at random and detached it from the rest. The bond was then reattached to a random site located on the main polymer so that the new vector connecting the new junction and the pasted monomer had one of the lengths specified above. If the repositioning resulted in two overlapping monomers or a reattachment to an existing

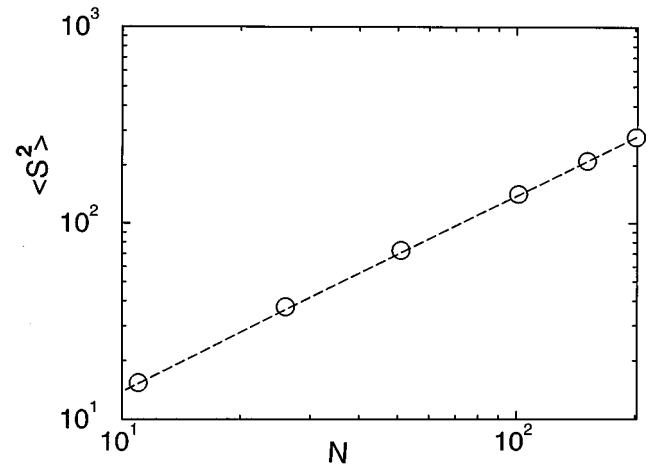


FIG. 2. Radius of gyration of randomly branched polymers $\langle S^2 \rangle$ vs the total number of monomers N . The straight line represents the asymptotic scaling behavior in Eq. (1) with $\nu=0.49 \pm 0.1$.

branching point, the move was rejected. This process was continued until an equilibrium state was obtained. From an initial straight-line configuration, a relaxed state could typically be reached within 5000 MC steps for even the largest structures of 200 monomers considered in this paper. After equilibration, positions of the monomers and the branching structure for five sample molecules were then recorded in intervals of 10^5 MC steps. This procedure allowed for the change of conformational and structural configurations before the next sample structure was adopted and ensured the structures were independent.

To confirm that the above algorithm indeed produces the desired branched structure in the lattice environment, we have examined scaling behavior of the radius of gyration and other conformation properties. As shown analytically by Parisi and Sourlas [9] and later confirmed numerically by van Rensburg and Madras [7] and Cui and Chen [6], the mean-square radius of gyration of an annealed randomly branched polymer should have the scaling behavior

$$\langle S^2 \rangle \equiv \frac{1}{N} \sum_{i=1}^N (\vec{R}_i - \vec{R}_c)^2 \sim N^{2\nu}, \quad (1)$$

where $\nu = \frac{1}{2}$ and \vec{R}_c is the center of mass. As shown by the plot in Fig. 2, the mean-square radius of gyration $\langle S^2 \rangle$ displays the power-law behavior cited above with exponent $\nu=0.49 \pm 0.01$, calculated from the last four points in the curve, which is consistent with these previous studies. Note that the relationship $\langle S^2 \rangle \approx N$ is the same as for linear polymers in the θ condition; the similarity is coincidental. We have also included in Table I other structural properties, such as the average number of branching monomers n_3 and the average number of “spacer” monomers between two branching monomers l . These data are comparable to the results from our earlier study [6] by using an off-lattice bead-bond algorithm for the case when the bead size equals the bond length.

To simulate the Rouse dynamics of the molecules, we started with five sample structures for each N constructed earlier. The branching structures were completely frozen so

TABLE I. Structurally averaged static properties.

N	$\langle S^2 \rangle$	n_3	l
11	15.4	2.15	
26	37.3	6.22	1.52
51	72.6	13.0	1.77
101	141.9	26.5	1.87
151	210.3	40.02	1.92
201	278.6	53.5	1.82

that every move only involved the displacement of a monomer chosen at random to one of the six possible neighboring sites according to the bond-fluctuation model [12]. The overall dynamics of these structures can be characterized by various time scales. The first is related to the translational and rotational diffusion of the entire polymer in the solvent medium (a long-time relaxation process). We also found that on a shorter time scale the polymers deform and reorganize their shape as the monomers move. This motion resembles the radial elastic deformation of a spherical elastic object. The autocorrelation function displays a nonexponential decay. In contrast, the internal relaxation of regularly branched polymers is usually associated with a simple exponential decay [10,11].

Throughout this paper, all measures of time are given in terms of MC steps, where one MC step consists of moving each of N randomly chosen monomers once. The ideal treatment for determining an autocorrelation function would be to divide the simulation into many segments; within each segment one would observe the system for a substantial amount of time, during which all relaxation processes would have time to complete. Then one would treat the starting point of each of these segments as if they were different members of a statistical ensemble; the ensemble average (denoted by $\langle \rangle$ below) would be performed over all of these segments of the simulation. In reality, however, due to limited computational time, we used an overlapping method to perform the ensemble average. The overlap is, however, sufficiently small so that correlations between frames are not significant. Table II shows the parameters used to calculate the autocorrelation function for each sample structure. The second column represents the total MC steps used for each run, in units of 10^6 MC steps. The third column represents the time interval after which a new configuration is considered for the ensemble average. The starting points of the overlapping segments were separated by time intervals that were longer than the elastic relaxation times to be discussed below. The last column represents the time duration for which the autocorrelation functions were observed for their time dependences.

TABLE II. Measurement parameters.

N	Total MC steps	Time interval	Time duration of observation
11	100M	2500	25 000
26	100M	5000	25 000
51	200M	20 000	100 000
101	500M	50 000	200 000

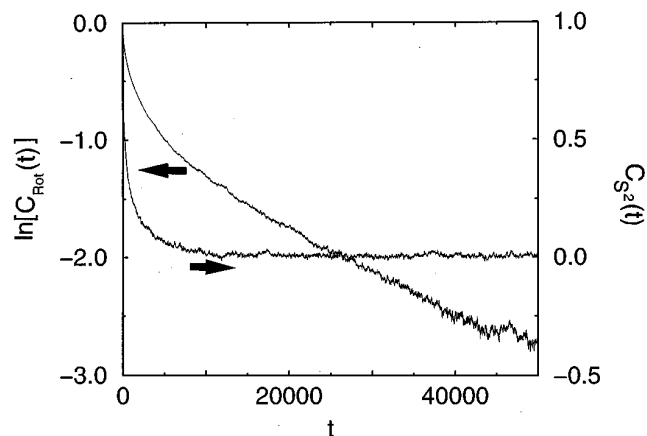


FIG. 3. Autocorrelation function $C_{\text{rot}}(t)$ vs t for $N=51$ on a semilogarithmic plot (to the left scale). Note that the long-time behavior is essentially linear. An overlay of $C_{S^2}(t)$ for $N=51$ is also included (to the right scale).

The calculations required for this study are substantial. For example, since each sample structure requires 5×10^8 MC steps for an $N=101$ molecule, the total time used to calculate the correlation functions for the five structures amounts to 25×10^8 MC steps. The actual calculations were performed on a 175-MHz Silicon Graphics INDY workstation.

The translational motion of the polymer is easily characterized through a direct measurement of the diffusion rate associated with the correlation function of the center-of-mass vector \vec{R}_c ,

$$C_{\text{diff}}(t) = \langle [\vec{R}_c(t) - \vec{R}_c(0)]^2 \rangle \equiv Dt. \quad (2)$$

The last step defines the diffusion constant D . Qualitatively, we expect that the diffusion constant displays the characteristic relation $D \propto 1/N$ of a Rouse model. Our data agree with this scaling relation. To measure the rotational relaxation time, we used the correlation function of the end-to-end vector \vec{R}_e ,

$$C_{\text{rot}}(t) = \frac{\sum_i^M \langle \vec{R}_i(t) \cdot \vec{R}_i(0) \rangle}{\sum_i^M \langle \vec{R}_i^2 \rangle}, \quad (3)$$

where \vec{R}_i is a vector that starts from a prior chosen external monomer to another external monomer. The sum is taken over all other external monomers, with M the number of free external ends. Figure 3 displays the rotational correlation function $C_{\text{rot}}(t)$ for $N=51$, plotted against a semilogarithmic scale on the left. There is a short period of nonexponential behavior in the initial portion of the curve, which has a time scale comparable to the elastic time scale to be discussed below. We believe that this is caused by a direct coupling to the internal relaxation of the structure that defines the shorter-time scales. The curve to the right scale in Fig. 3 shows an overlay of the correlation function for the change in the magnitude of S^2 for $N=51$, clearly demonstrating the

TABLE III. Rotational relaxation parameters.

N	τ_{rot}	τ_{rot}/N^2	τ_{rot}/NS^2
11	930 ± 94	7.7 ± 1	39 ± 1
26	6100 ± 250	9.0 ± 0.5	38 ± 2
51	$28\,000 \pm 2800$	10.8 ± 1	42 ± 4
101	$110\,000 \pm 29\,000$	10.8 ± 3	41 ± 10

relation between the nonexponential portion of the rotation curve and the internal relaxation of the structure. The crossover to the long-time exponential behavior occurs after the internal dynamic relaxation completes. Note that the initial portion of the relaxation curve might mislead the analyst. One could, for example, try to identify the initial portion of the $C_{\text{rot}}(t)$ curve with a stretched exponential decay by mistake. In order to find the true relaxation behavior, we observed $C_{\text{rot}}(t)$ until the long-time behavior clearly displayed a dominating simple exponential behavior. The rotational process of the whole polymer is always accompanied by the internal reorganization of the monomers. It is not until the process of reorganization has proceeded sufficiently that correlations from activities such as the twisting and untwisting of free ends become insignificant and the expected exponential decay behavior is observed. The relaxation time was calculated from the exponential part according to

$$\ln[C_{\text{rot}}(t)] = \text{const} - \left(\frac{1}{\tau_{\text{rot}}}\right)t. \quad (4)$$

A very simple physical picture can be proposed to relate the rotational time to the diffusion constant [10]. Since the rotational relaxation time should be approximately equal to the time required for the polymer to diffuse through a distance of its own diameter, characterized by the radius of gyration S , we can estimate the rotational relaxation time

$$\tau_{\text{rot}} \sim S^2/D \sim S^2N \sim N^2. \quad (5)$$

We have listed in columns 3 and 4 of Table III the combinations τ_{rot}/N^2 and $\tau_{\text{rot}}/(NS^2)$. Approaching a constant for large N , these data confirm the expected scaling relation in Eq. (5). It can also be seen that the smaller polymers ($N = 11$) produce a relatively small τ_{rot}/N^2 compared to the other values in the third column. Since the scaling relation $S^2 \sim N$ does not hold for smaller polymers, the combination S^2N is a better estimate for τ_{rot} , as seen in the fourth column of Table III.

The shorter-time scale dynamics of the polymer was another phenomenon of interest in this numerical study. In order to obtain a complete picture of the relaxation process of different components in the molecule, three aspects of the polymer were examined. The most important one is a measure of the relaxation of the squared radius of gyration

$$C_{S^2}(t) = \frac{\langle S^2(t)S^2(0) \rangle - \langle S^2 \rangle^2}{\langle S^4 \rangle - \langle S^2 \rangle^2}, \quad (6)$$

which provides a measure of the internal deformation of the entire structure. To gain insight into the role that branched monomers play in the internal dynamics of the polymer, we

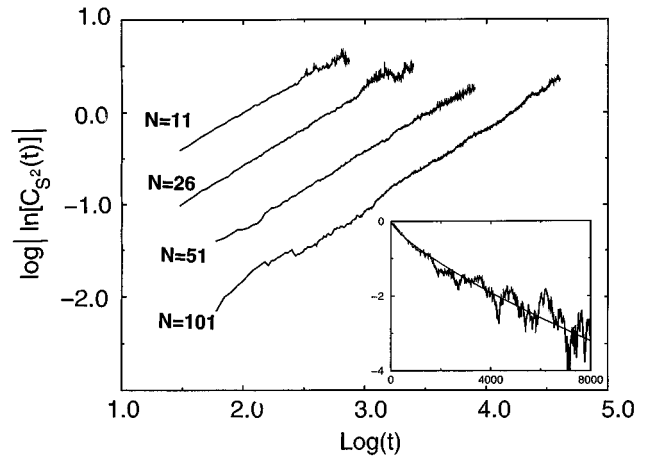


FIG. 4. Typical double-logarithmic plot for the correlation function of S^2 [Eq. (6)], where $\log(t)$ means $\log_{10}(t)$.

introduce a correlation function that measures the change in the radius of gyration of the branching monomers S_b ,

$$C_b(t) = \frac{\langle S_b^2(t)S_b^2(0) \rangle - \langle S_b^2 \rangle^2}{\langle S_b^4 \rangle - \langle S_b^2 \rangle^2}, \quad (7)$$

where

$$S_b^2 \equiv \frac{1}{n_3} \sum_{i=1}^{n_3} (\vec{R}_i^b - \vec{R}_c)^2 \quad (8)$$

and \vec{R}_i^b is the position of the i th branching point and n_3 the number of branching points of a given configuration. The third autocorrelation function is for the change in the square of the magnitude of the end-to-end vector \vec{R}_e ,

$$C_e(t) = \frac{\langle R_e^2(t)R_e^2(0) \rangle - \langle R_e^2 \rangle^2}{\langle R_e^4 \rangle - \langle R_e^2 \rangle^2}, \quad (9)$$

where

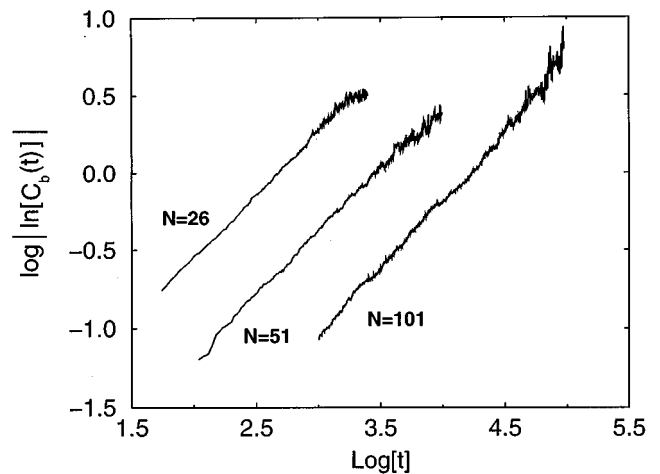


FIG. 5. Typical double-logarithmic plot of the correlation function of S_b^2 [Eq. (7)], where $\log(t)$ means $\log_{10}(t)$.

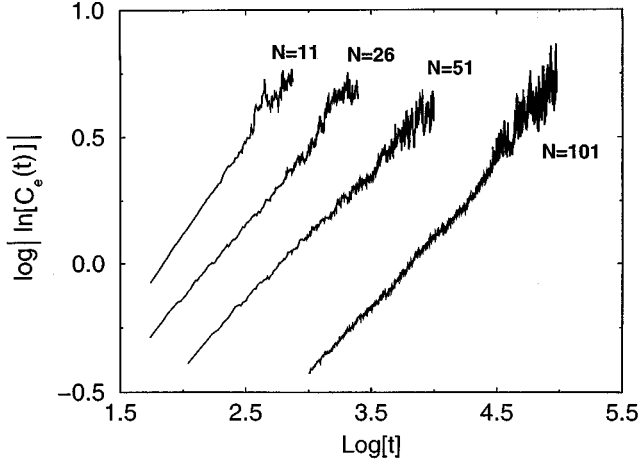


FIG. 6. Typical double-logarithmic plot of the correlation function of R_e^2 [Eq. (9)], where $\log(t)$ means $\log_{10}(t)$.

$$R_e^2 = \frac{1}{M} \sum_{i=1}^M (\vec{R}_i^{\text{end}} - \vec{R}_0^{\text{end}})^2 \quad (10)$$

and \vec{R}_i^{end} is the position vector of the i th free end of the polymer, \vec{R}_0^{end} the position vector of the center of mass of the M external ends, and M the number of free ends. This function provides a measurement of the relaxation process associated with the linear segments between the free ends.

These correlation functions reflecting internal dynamics are nonexponential in nature. In particular we propose fitting the correlation functions using stretched exponential decaying functions

$$C(t) = \exp\left[-\left(\frac{t}{\tau}\right)^\alpha\right]. \quad (11)$$

This assumption is based on the observations of Figs. 4–6, which show that the correlation functions C_{S^2} , C_b , and C_e in double logarithmic plots display linear behavior. The results of the data analysis are presented in Table IV. To further stress that the observed autocorrelation function is of a nonexponential nature, we have included in Fig. 4 an inset that displays a typical $C_{S^2}(t)$ curve ($N=51$) on a semilogarithmic scale.

The short relaxation time and the stretching exponents were determined from a least-squares fit of the simulation data in Figs. 4–6 to Eq. (11). The α 's for $C_{S^2}(t)$ and $C_b(t)$ have similar values, ranging from 0.62 to 0.95 depending on the particular branching structure. The correlation function for the end monomers $C_e(t)$, however, decays much faster, with a smaller stretching exponent α ranging from 0.50 to

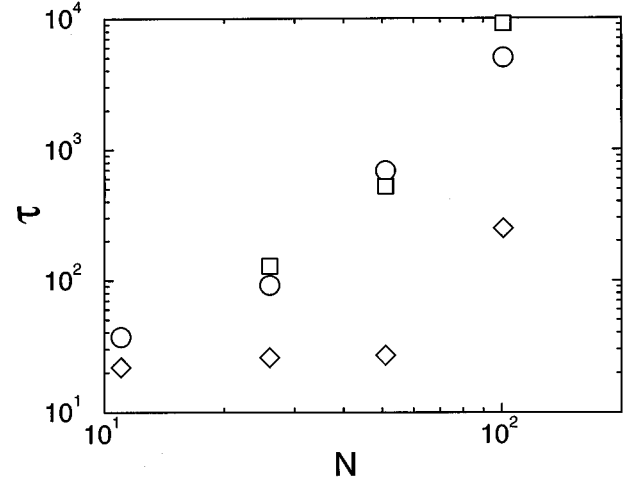


FIG. 7. Elastic relaxation times τ_{S^2} (circles), τ_b (squares), and τ_e (diamonds) as functions of N , averaged over the five representative structures.

0.82. The structurally averaged decay times for these three correlation functions are also listed in Table IV. The shorter decay times for $C_e(t)$ reflect the fact that external monomers move more freely with fewer constraints. The overall elastic relaxation of the polymer involves the combined effects of the free ends, branched monomers, and linear parts between the branched monomers. Constrained by extra bonding, the branching monomers are less mobile, having the slowest internal relaxation process among the three. Thus the relaxation process of S^2 is dominated mainly by that of the branching monomers.

In an attempt to determine possible scaling relations, we have plotted the short relaxation times vs the number of monomers in Fig. 7 using a double-logarithmic scale. It appears from this plot that

$$\tau_{S^2} \propto \tau_b \propto N^{(3 \pm 0.2)}. \quad (12)$$

Since the N used here is not sufficiently large, we are unable to make a conclusive estimate for the corresponding scaling exponent. The accuracy of these data points is further hampered by the determination of the α exponents, which already carry relatively large error bars. These statistical errors were estimated from combining the original statistical errors associated with the fitting of the double exponential curve for each given structure and the statistical errors associated with the structural averaging.

The scaling behavior for the short-time scale dynamics observed in this study is not fully understood. Though the simulation data were fitted to the stretched exponential function in Eq. (11), the actual time dependence of these corre-

TABLE IV. Elastic relaxation parameters.

N	τ_{S^2}	α_{S^2}	τ_b	α_b	τ_e	α_e
11	37 ± 3	0.62–0.83			22 ± 2	0.70–0.82
26	92 ± 8	0.70–0.90	130 ± 10	0.77–0.95	26 ± 4	0.51–0.70
51	690 ± 130	0.72–0.92	520 ± 80	0.69–0.88	27 ± 4	0.50–0.60
101	5000 ± 500	0.82–0.90	9100 ± 500	0.80–0.91	250 ± 60	0.55–0.61

lation functions is still debatable. It is therefore desirable to analyze the relaxation process in more detail by an analytic treatment. Even a calculation of the dynamical behavior of randomly branched polymers in the θ condition would clarify the underlying physics: The nonexponential behavior would already show up due to the random distribution of the segmental lengths.

A number of other randomly disordered systems also display nonexponential relaxation dynamics. The autocorrelation functions of these systems were also fitted to the stretched exponential formula. Ogielski has conducted an extensive investigation of the nonexponential nature of the autocorrelation function of the order parameter for spin-glass systems. The stretching exponent was shown to have various values smaller than unity, depending on the temperature [3]. A more closely related example is probably the dynamics of a linear heteropolymer chain, which relaxes from a near-equilibrium state to a "native" state according to a stretching exponent ranging from 0.38 to 0.54 [4].

There has been a great deal of research (see, for example, references in Ref. [1]) into the dynamics of dilute sol solutions, which are systems that contain polydisperse (i.e., non-uniform distribution of N) RBP's [1]. However, there has been few experiments on the dynamics of a very dilute RBP

solution, in which the dynamics of a single RBP would be important. A NMR measurement, for example, could be useful to probe some of the nonexponential relaxation processes described in this paper.

In summary, the bond-fluctuation algorithm has proved to be an ideal model for recreating the Rouse dynamics of RBP's, simulating the conformational properties and the long-time scale dynamics that can be understood from other theoretical treatments. We have observed in the simulation that the scaling relationships $D \propto 1/N$ and $\tau_{\text{rot}} \propto N^2$ are valid for randomly branched polymers up to $N=101$. There are two important types of time scales. The long, rotational relaxation time is shown to obey the scaling behavior $\tau \propto N^2$. The results also show that the internal dynamics are nonexponential and are much faster, as demonstrated by the autocorrelation functions for the radius of gyration and the squared end-end distance. It also appears that these correlation functions may be represented by stretched exponential functions, with stretching exponents ranging from 0.50 to 0.95.

This work was supported by the Natural Science and Engineering Research Council of Canada. We would like to thank Philip Waldron for his critical reading of the manuscript.

-
- [1] For a review see, M. Daoud and A. Lapp, *J. Phys.: Condens. Matter* **2**, 4021 (1990), and references therein.
- [2] Also see P.G. de Gennes, *Biopolymers* **6**, 715 (1968); P. L. Privaloo and V. V. Filimonov, *J. Mol. Biol.* **122**, 447 (1978); P. G. Higgs, *J. Phys. (France) I* **3**, 43 (1993).
- [3] A. T. Ogielski, *Phys. Rev. B* **32**, 7384 (1985).
- [4] See, e.g., G. Iori, E. Marinari, and G. Parisi, *Europhys. Lett.* **25**, 491 (1994).
- [5] A. M. Gutin, A. Y. Grosberg, and E. I. Shakhnovich, *Macromolecules* **26**, 1293 (1993); *J. Phys. A* **26**, 1037 (1993).
- [6] S.-M. Cui and Z. Y. Chen, *Phys. Rev. E* **52**, 5084 (1995); **52**, 3943 (1995); **53**, 6238 (1996).
- [7] E. J. van Rensbury and N. Madras, *J. Phys. A* **25**, 303 (1992), and references therein.
- [8] T. C. Lubensky and J. Isaacson, *Phys. Rev. A* **20**, 2130 (1979); J. Isaacson and T. C. Lubensky, *J. Phys. (France) Lett.* **41**, L466 (1980).
- [9] G. Parisi and N. Sourlas, *Phys. Rev. Lett.* **46**, 871 (1981).
- [10] G. Grest and M. Murat, in *Monte Carlo and Molecular Dynamics Simulations in Polymer Science*, edited by K. Binder (Oxford University Press, New York, 1995).
- [11] S.-J. Su, M. S. Denny, and Kovac, *Macromolecules* **24**, 917 (1991).
- [12] M. Doi and S. F. Edwards, *The Theory of Polymer Dynamics* (Clarendon, Oxford, 1986); H. Yamakawa, *Modern Theory of Polymer Solutions* (Harper and Row, New York, 1971).
- [13] B. H. Zimm and R. W. Kilb, *J. Polym. Sci.* **37**, 19 (1959).
- [14] C. Cai and Z. Y. Chen, *Macromolecules* **30**, 5102 (1997).
- [15] I. Carmesin and K. Kremer, *Macromolecules* **21**, 2819 (1988); *J. Phys. (France)* **51**, 915 (1990).